SCIENCE CHINA
Physics, Mechanics & Astronomy

• Article •

September 2023 Vol. 66 No. 9: 290313
https://doi.org/10.1007/s11433-023-2147-3

Optical experimental solution for the multiway number partitioning problem and its application to computing power scheduling

Jingwei Wen[1*], Zhenming Wang[2], Zhiguo Huang[1], Dunbo Cai[1], Bingjie Jia[2], Chongyu Cao[2], Yin Ma[2], Hai Wei[2], Kai Wen[2*], and Ling Qian[1*]

[1] *China Mobile (Suzhou) Software Technology Company Limited, Suzhou 215163, China;*
[2] *Beijing QBoson Quantum Technology Co., Ltd., Beijing 100015, China*

Received April 1, 2023; accepted May 23, 2023; published online August 3, 2023

Quantum computing is an emerging technology that is expected to realize an exponential increase in computing power. Recently, its theoretical foundation and application scenarios have been extensively researched and explored. In this work, we propose efficient quantum algorithms suitable for solving computing power scheduling problems in the cloud-rendering domain, which can be viewed mathematically as a generalized form of a typical NP-complete problem, i.e., a multiway number partitioning problem. In our algorithm, the matching pattern between tasks and computing resources with the shortest completion time or optimal load balancing is encoded into the ground state of the Hamiltonian; it is then solved using the optical coherent Ising machine, a practical quantum computing device with at least 100 qubits. The experimental results show that the proposed quantum scheme can achieve significant acceleration and save 97% of the time required to solve combinatorial optimization problems compared with classical algorithms. This demonstrates the computational advantages of optical quantum devices in solving combinatorial optimization problems. Our algorithmic and experimental work will advance the utilization of quantum computers to solve specific NP problems and will broaden the range of possible applications.

quantum algorithm, coherent Ising machine, multiway number partitioning problem

PACS number(s): 03.67.-a, 03.67.Lx, 03.65.Ta

Citation: J. Wen, Z. Wang, Z. Huang, D. Cai, B. Jia, C. Cao, Y. Ma, H. Wei, K. Wen, and L. Qian, Optical experimental solution for the multiway number partitioning problem and its application to computing power scheduling, Sci. China-Phys. Mech. Astron. **66**, 290313 (2023), https://doi.org/10.1007/s11433-023-2147-3

1 Introduction

The advancement of quantum technology is of great scientific significance and social value, which is expected to have a considerable impact on traditional technology and trigger a technological revolution and industrial transformation [1-4]. As the cutting edge of quantum technology, quantum computing is dedicated to using the principles of quantum mechanics to calculate and simulate complex systems [5-7]. Due to its potential advantages in processing large amounts of data quickly and efficiently, quantum computers are expected to play an important role in secure encryption [8, 9], database search [10, 11], machine learning [12, 13], and many other scenarios that are intractable with classical computers [14-20].

*Corresponding authors (Jingwei Wen, email: wjw17@tsinghua.org.cn; Kai Wen, email: wenk@boseq.com; Ling Qian, email: qianling@cmss.chinamobile.com)

People can quickly optimize the scheduling processes of personnel and equipment to maximize efficiency and minimize costs in scenarios such as communication networks [21, 22], healthcare [23], transportation [24-26], and complex supply chain management [27-32] by harnessing the power of quantum computers. Furthermore, quantum computing has the potential to revolutionize the field of computing power scheduling in cloud computing [33-35], which requires searching a large solution space for the optimal configurations for allocating computing resources to various tasks with improved performance and efficiency.

This paper focuses on a particular application scenario regarding the computing power scheduling problem in a cloud-rendering domain, which can be mathematically modeled as a generalized form of the multiway number partitioning problem, a critical NP-complete problem [36-44]. Herein, two quantum algorithms from different optimization viewpoints are proposed, and an experimental solution on the optical coherent Ising machine (CIM) is presented [45-53], which is an over 100-qubit quantum computing device. The experimental results show that our quantum scheme can realize a significant quantum acceleration, saving 97% of solving time on average compared with classical simulated annealing (SA) and tabu search algorithms [54]. Being the first experimental demonstration of a quantum algorithm for the generalized multiway number partitioning problem in optical systems, our paper presents the acceleration of quantum computers relative to classical techniques for a specific NP-complete problem and discusses a new application scenario for quantum computing.

This paper is organized as follows: we begin with some preliminary material in sect. 2, followed by a description of the proposed quantum algorithms in sect. 3, which transform the scheduling of computing power resources into an optimization problem. Sect. 4 presents an experimental demonstration of the quantum algorithm on a practical optical quantum computer, as well as comparisons with classical algorithms. Finally, we conclude in sect. 5.

2 Preliminaries

2.1 Background and mathematical reduction

The task of computing power scheduling for image rendering is a crucial process in cloud computing [55], as shown in Figure 1. In general, such a scenario is as follows: the client submits a rendering task with specific requirements, and the service providers must find the optimal schemes to invoke computing resources. The basic idea is to find the fewest number of servers possible while keeping constraints in mind. This is accomplished by first presenting a machine number and then applying various heuristic algorithms to determine the current state (completion time, load balancing, and so on) for comparing satisfaction. However, due to a growing volume of data, the optimal task-server scheduling scheme cannot be effectively obtained in large-scale dynamic cloud rendering, and redundant rendering is a common phenomenon. This would result in a mismatch between server and rendering tasks, wasting computing resources and reducing rendering efficiency.

Mathematically, this procedure can be modeled as a generalized multiway number partitioning problem [42-44], which is an example of an NP-complete problem [37]. The multiway number partitioning problem is defined as dividing/partitioning a given set $S = \{\cdots, a_i, \cdots\}$ of positive integers into k subsets to make the sum of subsets as equal as possible. For the widely studied $k = 2$ case, the number partitioning problem (NPP) can be characterized as an optimization problem to mitigate the difference $D_{(2)} = \left|\sum_{a_i \in A} a_i - \sum_{a_i \in S \setminus A} a_i\right|$ between subset A and complementary set $S \setminus A$ [40,41]. Generally, if we set the arbitrary k subsets as $A_k \subset S$ satisfying $\cup_k A_k = S$ and $A_k \cap A_{k'} = \emptyset$ for $k \neq k'$, the optimization function to be minimized can be reformulated as:

$$D_{(k)} = \sum_{k \neq k'} \Big| \sum_{a_i \in A_k} a_i - \sum_{a_i \in A_{k'}} a_i \Big|. \tag{1}$$

Here, we extend the balanced bipartition ($k = 2$) to multipartitioned cases ($k \geq 2$) without restricting the elements to integers. Furthermore, the target sum of each subset can be set differently, resulting in the partitioning of the set S into several subsets with unequal sums. Using these extensions, we can establish a correspondence between such a generalized multiway NPP and computing power scheduling problem in the cloud-rendering domain, as detailed in sect. 3.

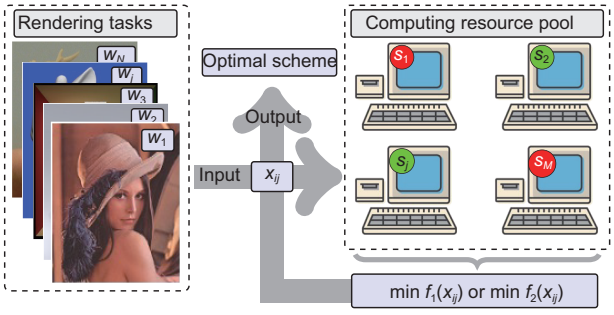

Figure 1 (Color online) Schematic of the cloud-rendering computing power scheduling process. There are N tasks in the queue to be assigned to M machines, and each machine processes one task at a time. The expected duration of task $i \in \{1, 2, \cdots, N\}$ is w_i and the beginning of available time for machine $j \in \{1, 2, \cdots, M\}$ is s_j. The scheduling scheme is encoded in a series of binary variables (x_{ij}), and the best objective schemes can be found by minimizing the proposed optimization functions $f_1(x_{ij})$ in eq. (8) with minimum completion time or $f_2(x_{ij})$ in eq. (10) with best load balancing.

2.2 QUBO and Ising model

The quadratic unbounded binary optimization (QUBO) problem and its relationship with the Ising model are introduced briefly here. Many canonical NP-hard and NP-complete problems have been shown to be transformable into a combinatorial optimization form [56]. A large class of these optimization problems can be expressed in QUBO form with binary variables of $\{0,1\}$ basis or in $\{-1,1\}$ basis with spin variables of the Ising model, and these two forms with different bases are interchangeable [57]. Specifically, the mathematical form of the QUBO problem is demonstrated as follows:

$$f_{\mathrm{QUBO}}(x) = \sum_{i\leq j} q_{ij}x_i x_j = x^{\mathrm{T}}Qx, \tag{2}$$

where $x = \{x_i\}$ is the binary variable vector to be solved, and the QUBO matrix $Q = \{q_{ij}\}$ indicates the quadratic coefficients. The objective solution is

$$x^* = \arg\min_x f_{\mathrm{QUBO}}(x). \tag{3}$$

By transforming variables as $x_i \to (I+\sigma_i)/2$ where the σ_i is a spin variable, the optimization functions can be demonstrated with an Ising model. The target solution is then encoded in the ground states of the Hamiltonian:

$$H_{\mathrm{Ising}}(\sigma) = -\sum_{i,j} J_{ij}\sigma_i\sigma_j - \sum_i h_i\sigma_i, \tag{4}$$

where J_{ij} and h_i are the quadratic and linear coefficients, respectively. In our experimental system, the optical CIM platform can map the target QUBO problem to an all-to-all connectivity Ising Hamiltonian with programmable parameters, and the optimal solution is obtained via controllable quantum phase transition processes.

Below, we present two quantum optimization algorithms that model the computing power scheduling (generalized multiway number partitioning) problem as a QUBO problem, along with an optical experimental demonstration and comparisons to classical algorithms.

3 Algorithms

In this section, we propose two quantum algorithms that describe the generalized multiway NPP as a QUBO problem from different optimization perspectives, using scheduling processes in the cloud-rendering domain as a specific example.

To begin, we define a set of binary variables x_{ij} to represent the state of matching between N tasks and M machines. Specifically, we set $x_{ij} = 1$ if task $i \in \{1,2,\cdots,N\}$ is completed/started on machine $j \in \{1,2,\cdots,M\}$, and $x_{ij} = 0$ otherwise. The expected duration of task i serves as a weight number w_i, and the total time of tasks are $\mathcal{W} = \sum_{i=1}^{N} w_i$. The completion time for tasks performing on machine j is $c_j = \sum_{i=1}^{N} w_i x_{ij} + s_j$, where s_j is the idle start time for machine j, satisfying $\sum_{j=1}^{M} s_j = \mathcal{S}$. To ensure that task i is assigned to only one machine, we can add a constraint as follows:

$$\sum_{j=1}^{M} x_{ij} = 1. \tag{5}$$

After that, we have $\sum_{j=1}^{M} c_j = \mathcal{W} + \mathcal{S}$. To begin, we propose an optimization function for minimizing the overall task completion time, which is equivalent to determining the minimum of the maximum (min-max) values of c_j:

$$\min_{x_{ij}} \max_j \{c_1, c_2, \cdots, c_j, \cdots, c_M\}. \tag{6}$$

By introducing variable u with $u \geq c_j \ \forall j$, the original problem can be changed to find the minimum values of an optimization function $\min f_1(x_{ij}) = \min u$. Then, the inequality can be transformed into equality using slack-variables $v_j^{(s)} = u - c_j \ \forall j$, and they can be expressed using binary expansion as:

$$u = \sum_{l=0}^{L-1} 2^l u_l^{(s)} \geq 0, \ v_j^{(s)} = \sum_{l=0}^{L-1} 2^l v_{jl}^{(s)} \geq 0, \tag{7}$$

where parameter L is linked to precision, while $u_l^{(s)}$ and $v_{jl}^{(s)}$ take values of zero or one. By incorporating all these constraints into the objective function, the optimization function for the min-max problem is obtained:

$$\begin{aligned} f_1(x_{ij}) = &\sum_{l=0}^{L-1} 2^l u_l^{(s)} + \beta_1 \sum_{i=1}^{N} \left(\sum_{j=1}^{M} x_{ij} - 1 \right)^2 \\ &+ \beta_2 \sum_{j=1}^{M} \left(\sum_{l=0}^{L-1} 2^l \left(u_l^{(s)} - v_{jl}^{(s)} \right) - \sum_{i=1}^{N} w_i x_{ij} - s_j \right)^2, \end{aligned} \tag{8}$$

where β_1 and β_2 are penalty coefficients. The total number of variables, in this case, is $(NM + L + ML)$. Because of the addition of slack variables, improving accuracy is dependent on increasing the number of encoding bits, which is incompatible with applying the algorithm to noisy intermediate-scale quantum devices.

Alternatively, we can turn to find the optimal scheme with a balanced load for each machine, which can be realized by searching a relatively balanced distribution of completion time [58]; furthermore, it can be transformed into locating the minimum values of a variance-like optimization function:

$$f_2(x_{ij}) = \frac{1}{M} \sum_{j=1}^{M} \left(c_j - \frac{\mathcal{W} + \mathcal{S}}{M} \right)^2. \tag{9}$$

When combined with the constraint in eq. (5), the loss function to be minimized is

$$f_2(x_{ij}) = \frac{1}{M}\sum_{j=1}^{M}\left(\sum_{i=1}^{N} w_i x_{ij} + s_j - \bar{c}\right)^2 + \beta\sum_{i=1}^{N}\left(\sum_{j=1}^{M} x_{ij} - 1\right)^2, \tag{10}$$

where the penalty coefficient is β and expected mean value is $\bar{c} = (\mathcal{W} + \mathcal{S})/M$. In comparison to optimization function $f_1(x_{ij})$, this variance-like optimization function $f_2(x_{ij})$ only requires MN variables, resulting in a significant reduction in bits/qubits [59]; moreover, it is more consistent with the definition of the multiway NPP. Therefore, we will use the latter objective function for the following experimental demonstration and discussion. Once the optimal $\{0, 1\}$ series for x_{ij} is obtained, the tasks to be performed in each machine can be determined. Both objective functions constructed here have the QUBO form, and the target solution encoded in the ground states can be obtained using quantum algorithms such as quantum annealing [60,61] and quantum approximate optimization algorithm [62] on quantum computers. In the following section, we provide an optical experimental solution based on CIM, which can be a good physical platform for the QUBO problem, and many large-scale problems have been solved using this system [46,47,50].

4 Experiment

In this section, we present an optical realization and solution to the aforementioned algorithm using CIM. As shown in Figure 2, the CIM system is a hybrid quantum computing platform using laser pulses in optical fibers as

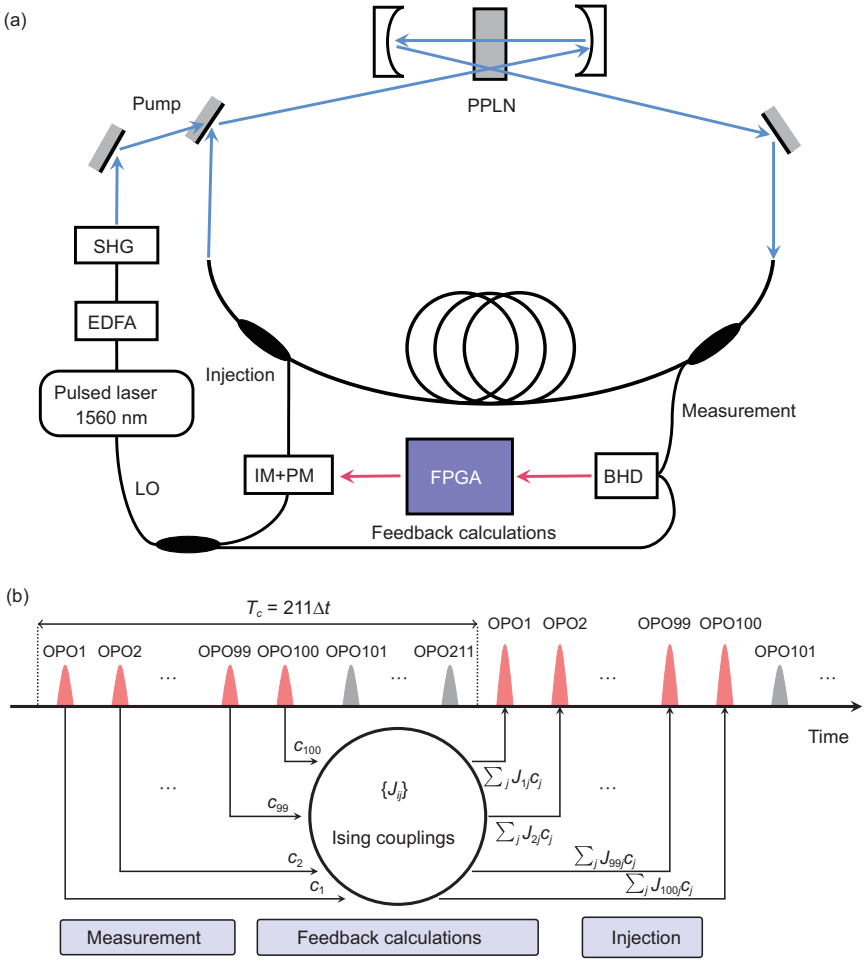

Figure 2 (Color online) Schematic of the measurement-feedback CIM. (a) EDFA stands for erbium-doped fiber amplifier, SHG stands for second harmonic generation, PPLN stands for periodically poled lithium niobate, BHD is the balanced homodyne detection, and IM/PM stands for intensity/phase modulator. The pulses of the local oscillator (LO) are directly obtained from the master laser. (b) The measurement-feedback subsystem. Only 100 of the 211 optical parametric oscillators (OPOs) are used as qubits, with the remaining pulses used to stabilize the system. The in-phase amplitude c_j ($j = 1, \cdots, 100$) is measured and used to compute the feedback signal for the next roundtrip. The time interval of each of the two pulses is $\Delta t = 10$ ns, and T_c indicates the transmission time of optical pulses in the loop.

qubits for computation, unlike traditional computers that use semiconductor-integrated chips. The optical quantum computer used here is a measurement-feedback CIM [45], which includes optical and electrical components and was developed by Beijing QBoson Quantum Technology Co., Ltd. (https://qboson.com). The CIM can effectively solve combinatorial optimization problems, and its benefits in the maximum cut (max cut) problem of fully connected 100000-node graphs have already been demonstrated in ref. [50].

Lasers, amplifiers, periodically poled lithium niobate (PPLN) crystals, and fiber rings make up the optical section. The laser is a femtosecond-pulsed fiber laser with a locked repetition frequency of 100 MHz. Because the laser output power (100 mW) is low, amplification is realized using an erbium-doped fiber amplifier (EDFA). Further, the frequency of the amplified laser is doubled using a PPLN crystal to produce a 780 nm laser, which is used as the pump source to synchronously pump the phase sensitive amplifier to form degenerate optical parametric oscillation (DOPO) [63-67]. There are 211 oscillating pulses in the fiber loop during the calculation, with a time interval of $\Delta t = 10$ ns between each of the two pulses. Therefore, the transmission time of optical pulses in the loop is $T_c = 2.11$ μs. Aside from the optical component, the electrical component includes a field-programmable gate array (FPGA), analog-to-digital/digital-to-analog (AD/DA) converter, and optical balanced homodyne detectors (BHD). The laser output in the fiber ring and the laser of fundamental frequency (1560 nm) are determined by an optical BHD, which can read out the in-phase amplitude c_j ($j = 1, \cdots, 100$) of output pulses. Then, these measurement results are used by the FPGA to compute the feedback signal for the next roundtrip based on the interaction intensity J_{ij} between spin i and spin j in the target Ising Hamiltonian. The Xilinx FPGA used here is capable of supporting digital signal processing multipliers and on-chip resource storage. Specifically, the feedback for the k-th pulse is $\sum_{j=1}^{N=100} J_{kj}c_j$, and the amplitude of this real-valued quantity is used as the control signal of the intensity modulator (IM), and its sign defines whether the phase modulator (PM) applies a 0 or a π phase shift.

To test the hardware capability, we run experiments with cases up to one hundred qubits and design two groups of experimental schemes that fix the machine (or task) number while varying other parameters. The CIM used in the experiments has a fixed number of simultaneous oscillating pulses in the fiber ring for qubits. If the model problem scale is less than the available qubits, non-computing qubits will be used to stabilize the system. We assume that the time required for each task, as well as the idle time for each machine, are both positive integers taken from set $\mathcal{N}^+$. For comparison, classical algorithms such as SA and tabu search are adopted to solve the experimental models, which were run 100 times on a central processing unit (Intel Core i7-10750H, 2.60 GHz with 16-gigabyte random-access memory) in each problem setup for obtaining the mean values and standard deviations.

The normalized pump amplitude (NPA), defined as pump amplitude normalized by the pump threshold of a single isolated DOPO pulse, is displayed by gray dashed lines in Figure 3. A phase transition occurs when the power of the pump light is gradually increased to the oscillation threshold, and cut values increase with running time. The cut value used in this case is the score of the maximum cut problem, which is transformed from the original optimization problem [50], and it is an antilinear measure to the objective function value; that is, maximization of cut corresponds to the minimization of the objective function. Then, the light transforms from squeezed vacuum states to coherent states with phases 0 and π, corresponding to spin states. The loss of such a specific single-mode oscillation is minimal and corresponds to the Ising Hamiltonian ground state. Figure 4 depicts the experimental spin/binary variable results with problem scales $[N, M] = [10, 4]$ and $[20, 5]$, respectively. The red nodes indicate $+1$ ($x_{ij} = 1$) and blue nodes imply -1 ($x_{ij} = 0$) for spins. Thus, we can conclude that the nearly all-connected graphs are complicated with high optimization complexity, and experimental output results meet the constraints.

Because the labels $x_{ij} = 1$ in red nodes indicate that the task i is assigned to machine j, the optimal scheduling method can be obtained directly based on the experimental spin states, as shown in Figure 5. The optimal allocation scheme has a makespan of 17 and 45, corresponding to the minimum- and maximum-scale in the experimental setup, which can be obtained using quantum and tabu search

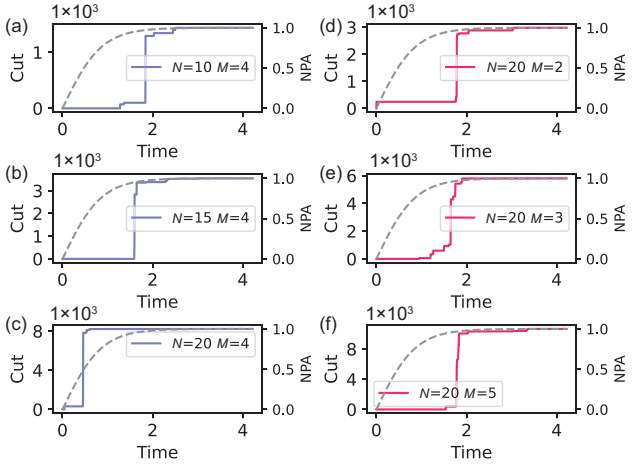

Figure 3 (Color online) Cut values with the running time (in milliseconds). The panels in the left column ((a)-(c)) set the number of machines to $M = 4$, whereas the panels in the right column ((d)-(f)) set the number of tasks to $N = 20$. The normalized pump amplitude (NPA) is represented by gray dashed lines.

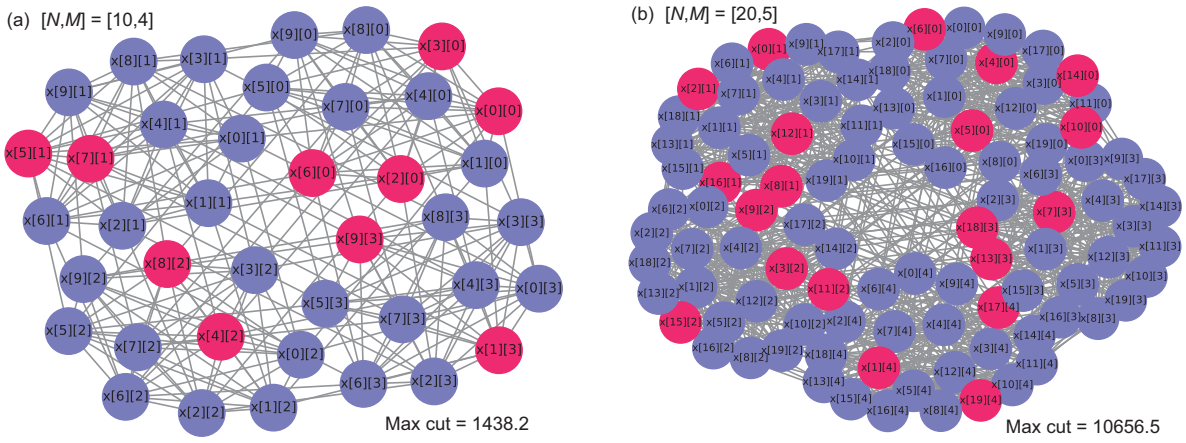

Figure 4 (Color online) Graphs and outcomes for experimental demonstration cases with minimum- and maximum-scales. (a) $[N, M] = [10, 4]$ and (b) $[N, M] = [20, 5]$. Notations $x[i][j] = x_{ij}$ here. The node colors represent different spin results, with red representing $+1$ and blue representing -1. The maximum cut value is also indicated.

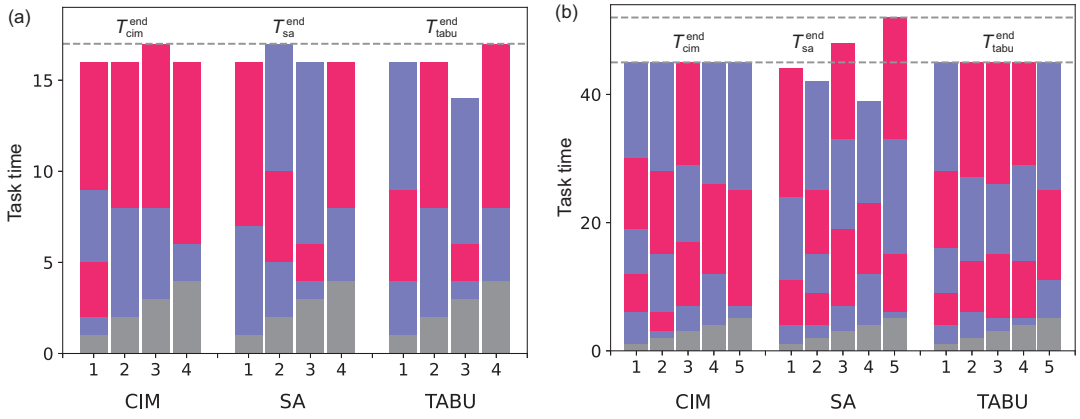

Figure 5 (Color online) Scheduling schemes established by quantum (CIM) and classical (SA and tabu) algorithms with different problem scales in the experiment. (a) $[N, M] = [10, 4]$ and (b) $[N, M] = [20, 5]$. The x-coordinate refers to different machines, while the lengths of the red and blue parts indicate the tasks allocated to each machine with corresponding durations, and the gray parts indicate the idle start time for each machine. The makespan ($T_{\text{cim}}^{\text{end}}$, $T_{\text{sa}}^{\text{end}}$ and $T_{\text{tabu}}^{\text{end}}$) of the entire task for various solutions are labeled by dashed lines.

algorithms. This demonstrates the feasibility and correctness of the quantum algorithm in solving the computing-power scheduling problem. Note that the optimal scheme is not unique because of the parameter setting, namely, the degeneracy of the ground state of the Ising Hamiltonian.

Furthermore, notations $t_{\text{sa/tabu/cim}}$ are introduced to represent the running time of various algorithms, which is depicted in Figure 6. A ratio between them is defined as follows:

$$R(\text{sa/tabu,cim}) = \frac{t_{\text{sa/tabu}} - t_{\text{cim}}}{t_{\text{sa/tabu}}} \tag{11}$$

to determine the time-saving (or acceleration) ability of the quantum algorithm. Given that the CIM solution is quick, a high ratio of $R(\text{sa/tabu,cim}) \in (0, 1)$ represents a huge quantum acceleration effect. The CIM solver is concluded to be faster than classical algorithms, with an average $R(\text{sa,cim}) = 96.7\%$ and $R(\text{tabu,cim}) = 98.5\%$ time-saving over SA and tabu search algorithms, respectively. Another comparable but more intuitive measure is introduced, namely, X-fold acceleration, which is defined as $X(\text{sa/tabu,cim}) = [1 - R(\text{sa/tabu,cim})]^{-1}$. On a 100 qubits scale, quantum solutions can achieve tens of times the acceleration of classical solutions, with $X(\text{sa,cim}) = 37.6$ and $X(\text{tabu,cim}) = 94.5$. We can also see that while the time of classical SA algorithm does not increase significantly with the scale of problem, it does so at the expense of accuracy, whereas the opposite is true for the tabu search algorithm. However, the quantum algorithm can guarantee the correctness and has a consistent running time of 2.37 ms on average. The solution time does not improve significantly for CIM with an increase in qubits; hence, greater advantages can be expected in large problem scales. Furthermore, optical quantum technology has the advantages of long coherence time at room temperature, scalability in space and time dimensions, and low power consumption

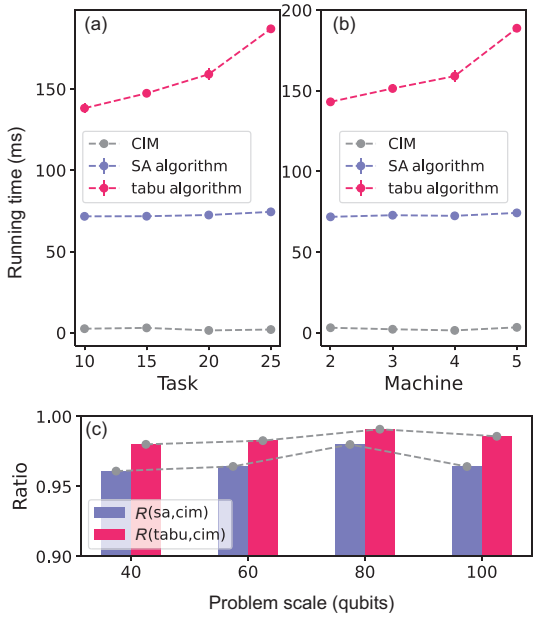

Figure 6 (Color online) Running time (in milliseconds) of the quantum algorithm based on CIM and two classical algorithms ((a), (b)) and the time-saving ratio R(sa/tabu,cim) with problem scale (c). The error bars of classical algorithms are calculated using the standard deviations of 100 repetitions. The machine number $M = 4$ is fixed in (a), whereas in (b), the task number is $N = 20$.

(600-800 W), which can considerably reduce the resource cost when compared with other quantum computing systems.

5 Conclusion

Although quantum computers have been shown to outperform classical computers in solving specific problems, developing quantum algorithms for important mathematical problems and actual production scenes remains an area of interest. In this paper, we propose two quantum algorithms from different optimization perspectives for solving computing power scheduling problems in the cloud-rendering domain, which can be mathematically modeled as the generalized multiway number partitioning ($k \geq 2$) problem, a typical NP-complete problem. Using a 100-qubit optical quantum computing system, the feasibility and advantage of the quantum algorithm are experimentally demonstrated, realizing an average of 96.7% and 98.5% time savings over classical SA and tabu search algorithms. The CIM-based quantum computing scheme has good accuracy and speed, and the running time remains relatively stable as the problem scale increases. Thus, it has an advantage in large-scale problems. Notably, multiway number partitioning is a fundamental problem, and many other problems, such as cryptography [40], can also be reduced to it mathematically. Therefore, our work considerably broadens the practical application scenarios of quantum computers based on hardware with tens of thousands of qubits [50] that is currently available.

This work was supported by the National Key R&D Plan (Grant No. 2021YFB2801800).

1 Y. Cao, J. Romero, J. P. Olson, M. Degroote, P. D. Johnson, M. Kieferová, I. D. Kivlichan, T. Menke, B. Peropadre, N. P. D. Sawaya, S. Sim, L. Veis, and A. Aspuru-Guzik, Chem. Rev. **119**, 10856 (2019).
2 D. Herman, C. Googin, X. Liu, A. Galda, I. Safro, Y. Sun, M. Pistoia, and Y. Alexeev, arXiv: 2201.02773.
3 F. Tennie, and T. Palmer, arXiv: 2210.17460.
4 S. Yarkoni, E. Raponi, T. Bäck, and S. Schmitt, Rep. Prog. Phys. **85**, 104001 (2022), arXiv: 2112.07491.
5 R. P. Feynman, *Simulating Physics with Computers: Feynman and Computation* (CRC Press, Boca Raton, 2018), pp. 133-153.
6 P. Benioff, J. Stat. Phys. **22**, 563 (1980).
7 S. Lloyd, Science **273**, 1073 (1996).
8 P. W. Shor, SIAM Rev. **41**, 303 (1999).
9 P. W. Shor, and J. Preskill, Phys. Rev. Lett. **85**, 441 (2000), arXiv: quant-ph/0003004.
10 L. K. Grover, Phys. Rev. Lett. **79**, 325 (1997), arXiv: quant-ph/9706033.
11 G. L. Long, Phys. Rev. A **64**, 022307 (2001), arXiv: quant-ph/0106071.
12 P. Rebentrost, M. Mohseni, and S. Lloyd, Phys. Rev. Lett. **113**, 130503 (2014), arXiv: 1307.0471.
13 H. Y. Huang, M. Broughton, M. Mohseni, R. Babbush, S. Boixo, H. Neven, and J. R. McClean, Nat. Commun. **12**, 2631 (2021), arXiv: 2011.01938.
14 A. Aspuru-Guzik, A. D. Dutoi, P. J. Love, and M. Head-Gordon, Science **309**, 1704 (2005), arXiv: quant-ph/0604193.
15 A. W. Harrow, A. Hassidim, and S. Lloyd, Phys. Rev. Lett. **103**, 150502 (2009), arXiv: 0811.3171.
16 B. Horstmann, B. Reznik, S. Fagnocchi, and J. I. Cirac, Phys. Rev. Lett. **104**, 250403 (2010), arXiv: 0904.4801.
17 F. Arute, K. Arya, R. Babbush, D. Bacon, J. C. Bardin, R. Barends, R. Biswas, S. Boixo, F. G. S. L. Brandao, D. A. Buell, B. Burkett, Y. Chen, Z. Chen, B. Chiaro, R. Collins, W. Courtney, A. Dunsworth, E. Farhi, B. Foxen, A. Fowler, C. Gidney, M. Giustina, R. Graff, K. Guerin, S. Habegger, M. P. Harrigan, M. J. Hartmann, A. Ho, M. Hoffmann, T. Huang, T. S. Humble, S. V. Isakov, E. Jeffrey, Z. Jiang, D. Kafri, K. Kechedzhi, J. Kelly, P. V. Klimov, S. Knysh, A. Korotkov, F. Kostritsa, D. Landhuis, M. Lindmark, E. Lucero, D. Lyakh, S. Mandrá, J. R. McClean, M. McEwen, A. Megrant, X. Mi, K. Michielsen, M. Mohseni, J. Mutus, O. Naaman, M. Neeley, C. Neill, M. Y. Niu, E. Ostby, A. Petukhov, J. C. Platt, C. Quintana, E. G. Rieffel, P. Roushan, N. C. Rubin, D. Sank, K. J. Satzinger, V. Smelyanskiy, K. J. Sung, M. D. Trevithick, A. Vainsencher, B. Villalonga, T. White, Z. J. Yao, P. Yeh, A. Zalcman, H. Neven, and J. M. Martinis, Nature **574**, 505 (2019), arXiv: 1910.11333.
18 H. S. Zhong, H. Wang, Y. H. Deng, M. C. Chen, L. C. Peng, Y. H. Luo, J. Qin, D. Wu, X. Ding, Y. Hu, P. Hu, X. Y. Yang, W. J. Zhang, H. Li, Y. Li, X. Jiang, L. Gan, G. Yang, L. You, Z. Wang, L. Li, N. L. Liu, C. Y. Lu, and J. W. Pan, Science **370**, 1460 (2020), arXiv: 2012.01625.
19 Y. Wu, W. S. Bao, S. Cao, F. Chen, M. C. Chen, X. Chen, T. H. Chung, H. Deng, Y. Du, D. Fan, M. Gong, C. Guo, C. Guo, S. Guo, L. Han, L. Hong, H. L. Huang, Y. H. Huo, L. Li, N. Li, S. Li, Y. Li, F. Liang, C. Lin, J. Lin, H. Qian, D. Qiao, H. Rong, H. Su, L. Sun, L. Wang, S. Wang, D. Wu, Y. Xu, K. Yan, W. Yang, Y. Yang, Y. Ye, J. Yin, C. Ying, J. Yu, C. Zha, C. Zhang, H. Zhang, K. Zhang, Y. Zhang, H. Zhao, Y. Zhao, L. Zhou, Q. Zhu, C. Y. Lu, C. Z. Peng, X. Zhu, and J. W. Pan, Phys. Rev. Lett. **127**, 180501 (2021), arXiv: 2106.14734.
20 Q. Zhu, S. Cao, F. Chen, M. C. Chen, X. Chen, T. H. Chung, H. Deng, Y. Du, D. Fan, M. Gong, C. Guo, C. Guo, S. Guo, L. Han, L. Hong, H.

L. Huang, Y. H. Huo, L. Li, N. Li, S. Li, Y. Li, F. Liang, C. Lin, J. Lin, H. Qian, D. Qiao, H. Rong, H. Su, L. Sun, L. Wang, S. Wang, D. Wu, Y. Wu, Y. Xu, K. Yan, W. Yang, Y. Yang, Y. Ye, J. Yin, C. Ying, J. Yu, C. Zha, C. Zhang, H. Zhang, K. Zhang, Y. Zhang, H. Zhao, Y. Zhao, L. Zhou, C. Y. Lu, C. Z. Peng, X. Zhu, and J. W. Pan, Sci. Bull. **67**, 240 (2022), arXiv: 2109.03494.

21 J. Choi, S. Oh, and J. Kim, Appl. Sci. **10**, 7116 (2020).

22 J. Kim, Y. Kwak, S. Jung, and J.-H. Kim, in *Quantum scheduling for millimeter-wave observation satellite constellation: 2021 IEEE VTS 17th Asia Pacific Wireless Communications Symposium (APWCS)* (IEEE, Osaka, 2021), pp. 1-5.

23 K. Ikeda, Y. Nakamura, and T. S. Humble, Sci. Rep. **9**, 12837 (2019), arXiv: 1904.12139.

24 A. Crispin, and A. Syrichas, in *Quantum annealing algorithm for vehicle scheduling: 2013 IEEE International Conference on Systems, Man, and Cybernetics* (IEEE, Manchester, 2013), pp. 3523-3528.

25 T. Tran, M. Do, E. Rieffel, J. Frank, Z. Wang, B. O'Gorman, D. Venturelli, and J. Beck, in *A hybrid quantum-classical approach to solving scheduling problems: Proceedings of the International Symposium on Combinatorial Search, volume 7* (Tarrytown, 2016), pp. 98-106.

26 T. Stollenwerk, E. Lobe, and M. Jung, in *Flight gate assignment with a quantum annealer: Quantum Technology and Optimization Problems: First International Workshop, QTOP 2019, Munich, Germany, March 18, 2019* (Springer, Cham, 2019), pp. 99-110.

27 T. Zheng, and M. Yamashiro, Int. J. Adv. Manuf. Technol. **49**, 643 (2010).

28 D. Venturelli, D. Marchand, and G. Rojo, in *Job shop scheduling solver based on quantum annealing: Proceedings of ICAPS-16 Workshop on Constraint Satisfaction Techniques for Planning and Scheduling (COPLAS)* (London, 2016), pp. 25-34.

29 K. Kurowski, J. Węglarz, M. Subocz, R. Różycki, and G. Waligóra, in *Hybrid quantum annealing heuristic method for solving job shop scheduling problem: Computational Science—ICCS 2020: 20th International Conference, Amsterdam, The Netherlands, June 3-5, 2020, Proceedings, Part VI 20* (Springer, Cham, 2020), pp. 502-515.

30 S. Yarkoni, A. Alekseyenko, M. Streif, D. Von Dollen, F. Neukart, and T. Bäck, in *Multi-car paint shop optimization with quantum annealing: 2021 IEEE International Conference on Quantum Computing and Engineering (QCE)* (IEEE, Broomfield, 2021), pp. 35-41.

31 A. Pakhomchik, S. Yudin, M. Perelshtein, A. Alekseyenko, and S. Yarkoni, arXiv: 2205.04844.

32 M. Geitz, C. Grozea, W. Steigerwald, R. Stöhr, and A. Wolf, in *Solving the extended job shop scheduling problem with agvs—Classical and quantum approaches: Integration of Constraint Programming, Artificial Intelligence, and Operations Research: 19th International Conference, CPAIOR 2022, Los Angeles, CA, USA, June 20-23, 2022, Proceedings* (Springer, Cham, 2022), pp. 120-137.

33 M. Armbrust, A. Fox, R. Griffith, A. D. Joseph, R. Katz, A. Konwinski, G. Lee, D. Patterson, A. Rabkin, I. Stoica, and M. Zaharia, Commun. ACM **53**, 50 (2010).

34 S. Singh, and I. Chana, J. Grid. Comput. **14**, 217 (2016).

35 M. Kumar, S. C. Sharma, A. Goel, and S. P. Singh, J. Network Comput. Appl. **143**, 1 (2019).

36 S. K. Sahni, J. ACM **23**, 116 (1976).

37 M. R. Garey, and D. S. Johnson, *Computers and Intractability: A Guide to the Theory of NP-completeness* (W. H. Freeman, New York, 1980).

38 H. De Raedt, K. Michielsen, K. De Raedt, and S. Miyashita, Phys. Lett. A **290**, 227 (2001).

39 T. Graß, D. Raventós, B. Juliá-Díaz, C. Gogolin, and M. Lewenstein, Nat. Commun. **7**, 11524 (2016), arXiv: 1507.07863.

40 L. Asproni, D. Caputo, B. Silva, G. Fazzi, and M. Magagnini, Quantum Mach. Intell. **2**, 4 (2020).

41 G. Anikeeva, O. Marković, V. Borish, J. A. Hines, S. V. Rajagopal, E. S. Cooper, A. Periwal, A. Safavi-Naeini, E. J. Davis, and M. Schleier-Smith, PRX Quantum **2**, 020319 (2021), arXiv: 2009.05549.

42 R. E. Korf, in *Multi-way number partitioning: Twenty-First International Joint Conference on Artificial Intelligence* (San Francisco, 2009), pp. 538-543.

43 E. L. Schreiber, R. E. Korf, and M. D. Moffitt, J. ACM **65**, 1 (2018).

44 Y. Deller, S. Schmitt, M. Lewenstein, S. Lenk, M. Federer, F. Jendrzejewski, P. Hauke, and V. Kasper, arXiv: 2204.00340.

45 Y. Haribara, Y. Yamamoto, K.-i. Kawarabayashi, and S. Utsunomiya, arXiv: 1501.07030.

46 P. L. McMahon, A. Marandi, Y. Haribara, R. Hamerly, C. Langrock, S. Tamate, T. Inagaki, H. Takesue, S. Utsunomiya, K. Aihara, R. L. Byer, M. M. Fejer, H. Mabuchi, and Y. Yamamoto, Science **354**, 614 (2016).

47 T. Inagaki, Y. Haribara, K. Igarashi, T. Sonobe, S. Tamate, T. Honjo, A. Marandi, P. L. McMahon, T. Umeki, K. Enbutsu, O. Tadanaga, H. Takenouchi, K. Aihara, K. Kawarabayashi, K. Inoue, S. Utsunomiya, and H. Takesue, Science **354**, 603 (2016).

48 Y. Yamamoto, K. Aihara, T. Leleu, K. Kawarabayashi, S. Kako, M. Fejer, K. Inoue, and H. Takesue, npj Quantum Inf. **3**, 49 (2017).

49 Y. Yamamoto, T. Leleu, S. Ganguli, and H. Mabuchi, Appl. Phys. Lett. **117**, 160501 (2020), arXiv: 2006.05649.

50 T. Honjo, T. Sonobe, K. Inaba, T. Inagaki, T. Ikuta, Y. Yamada, T. Kazama, K. Enbutsu, T. Umeki, R. Kasahara, K. Kawarabayashi, and H. Takesue, Sci. Adv. **7**, eabh0952 (2021).

51 N. Mohseni, P. L. McMahon, and T. Byrnes, Nat. Rev. Phys. **4**, 363 (2022), arXiv: 2204.00276.

52 B. Lu, L. Liu, J. Y. Song, K. Wen, and C. Wang, AAPPS Bull. **33**, 7 (2023).

53 B. Lu, C. R. Fan, L. Liu, K. Wen, and C. Wang, Opt. Express **31**, 3676 (2023).

54 H. Youssef, S. M. Sait, and H. Adiche, Eng. Appl. Artif. Intell. **14**, 167 (2001).

55 S. Shi, and C. H. Hsu, ACM Comput. Surv. **47**, 1 (2015).

56 A. Lucas, Quantum Inf. Process. **18**, 203 (2019), arXiv: 1812.01789.

57 A. Lucas, Front. Phys. **2**, 5 (2014), arXiv: 1302.5843.

58 S. A. Khawatreh, Int. J. Adv. Comput. Sci. Appl. **9**, 24 (2018).

59 R. Korf, in *Objective functions for multi-way number partitioning: Proceedings of the International Symposium on Combinatorial Search*, volume 1 (2010), pp. 71-72.

60 B. Apolloni, N. Cesa-Bianchi, and D. De Falco, in *A numerical implementation of "quantum annealing": Stochastic Processes, Physics and Geometry: Proceedings of the Ascona-Locarno Conference* (World Scientific, Singapore, 1990), pp. 97-111.

61 A. Das, and B. K. Chakrabarti, Rev. Mod. Phys. **80**, 1061 (2008), arXiv: 0801.2193.

62 E. Farhi, J. Goldstone, and S. Gutmann, arXiv: 1411.4028.

63 Z. Wang, A. Marandi, K. Wen, R. L. Byer, and Y. Yamamoto, Phys. Rev. A **88**, 063853 (2013), arXiv: 1311.2696.

64 T. Inagaki, K. Inaba, R. Hamerly, K. Inoue, Y. Yamamoto, and H. Takesue, Nat. Photon. **10**, 415 (2016), arXiv: 1604.08288.

65 W. Qin, A. Miranowicz, P. B. Li, X. Y. Lü, J. Q. You, and F. Nori, Phys. Rev. Lett. **120**, 093601 (2018), arXiv: 1709.09555.

66 W. Qin, A. Miranowicz, H. Jing, and F. Nori, Phys. Rev. Lett. **127**, 093602 (2021), arXiv: 2101.03662.

67 W. Qin, A. Miranowicz, and F. Nori, Phys. Rev. Lett. **129**, 123602 (2022), arXiv: 2203.06892.